Neuron, Vol. 27, 561–572, September, 2000, Copyright ©2000 by Cell Press

Presenilin-Mediated Modulation of Capacitative Calcium Entry

Andrew S. Yoo,*‖ Isaac Cheng,*‖ Sungkwon Chung,† Tallessyn Z. Grenfell,* Hanmi Lee,† Eunju Pack-Chung,* Melissa Handler,‡ Jie Shen,‡ Weiming Xia,‡ Giuseppina Tesco,* Aleister J. Saunders,* Kai Ding,‡ Matthew P. Frosch,‡ Rudolph E. Tanzi,* and Tae-Wan Kim*§

*Genetics and Aging Research Unit
Department of Neurology
Massachusetts General Hospital
Harvard Medical School
Charlestown, Massachusetts 02129
†Department of Physiology
Sungkyunkwan University School of Medicine
Suwon 440-746
South Korea
‡Center for Neurologic Diseases
Brigham and Women's Hospital
Boston, Massachusetts 02115

Summary

We studied a novel function of the presenilins (PS1 and PS2) in governing capacitative calcium entry (CCE), a refilling mechanism for depleted intracellular calcium stores. Abrogation of functional PS1, by either knocking out PS1 or expressing inactive PS1, markedly potentiated CCE, suggesting a role for PS1 in the modulation of CCE. In contrast, familial Alzheimer's disease (FAD)–linked mutant PS1 or PS2 significantly attenuated CCE and store depletion–activated currents. While inhibition of CCE selectively increased the amyloidogenic amyloid β peptide (Aβ42), increased accumulation of the peptide had no effect on CCE. Thus, reduced CCE is most likely an early cellular event leading to increased Aβ42 generation associated with FAD mutant presenilins. Our data indicate that the CCE pathway is a novel therapeutic target for Alzheimer's disease.

Introduction

Inherited mutations in the genes encoding the homologous presenilin proteins (PS1 and PS2) account for up to 40% of the early-onset cases of familial Alzheimer's disease (FAD) (reviewed by Tanzi, 1998). Both PS1 and PS2 are polytopic membrane proteins containing eight putative transmembrane (TM) domains (Doan et al., 1996; Li and Greenwald, 1998) and localized to intracellular membranes (Cook et al., 1996; Kovacs et al., 1996; Kim et al., 2000). Although a majority of nascent full-length presenilins are rapidly degraded by proteasomes (Kim et al., 1997), a subset of the presenilins are stabilized and undergo regulated endoproteolysis (Thinakaran et al., 1996, 1998; Kim et al., 1997), yielding N- and C-terminal heterodimeric complexes (Seeger et al., 1997; Capell et al., 1998) that comprise functional units of the presenilins (Saura et al., 1999; Tomita et al., 1999).

The presenilins appeared to be required for the proteolytic processing of the amyloid β protein precursor (APP) to yield amyloid β peptide (Aβ) (i.e., γ-secretase cleavage) (De Strooper et al., 1998). It has been demonstrated that two TM aspartate residues (D257 and D385 in PS1; D263 and D366 in PS2) are individually critical for presenilin-associated γ-secretase activity as well as presenilin endoproteolysis (Steiner et al., 1999; Wolfe et al., 1999; Kimberly et al., 2000). In addition, functional presenilins are also essential for proteolytic processing and/or maturation of other select membrane proteins, including Notch (De Strooper et al., 1999; Struhl and Greenwald, 1999; Ye et al., 1999), TrkB, APLP2 (Naruse et al., 1998) and hIre1α (Niwa et al., 1999). Common molecular phenotypes of FAD-associated mutations in the presenilins include increased levels of the 42 amino acid version of Aβ (Aβ42) in AD patients (Scheuner et al., 1996) as well as transfected cell lines and transgenic animals expressing FAD mutant forms of PS1 or PS2 (Borchelt et al., 1996; Citron et al., 1996; Duff et al., 1996; Tomita et al., 1997; Oyama et al., 1998). Aβ42 is an initial species that is deposited into senile plaques (Iwatsubo et al., 1994) and aggregates more readily than Aβ40 (reviewed by Selkoe, 1998).

Fibroblasts of AD patients or transfected cells harboring FAD mutant presenilins also exhibit altered cellular properties in relation to intracellular Ca^{2+} homeostasis. One of the most consistent effects of presenilin FAD mutations on Ca^{2+} signaling is the potentiation of IP_3-mediated release of Ca^{2+} from the internal store (Ito et al., 1994; Gibson et al., 1996; Guo et al., 1996; Etcheberrigaray et al., 1998; Leissring et al., 1999). However, the exact contribution of the presenilins on the intracellular Ca^{2+} signaling pathway has never been fully elucidated. Moreover, a molecular connection between this Ca^{2+}-related phenotype and other presenilin FAD phenotypes, such as increased Aβ42 generation, remains unresolved. Since the Aβ42-promoting effect of FAD mutant presenilins does not appear to be cell type specific (Borchelt et al., 1996; Duff et al., 1996; Citron et al., 1996; Scheuner et al., 1996; Tomita et al., 1997; Xia et al., 1997; Oyama et al., 1998), we set out to examine the normal and pathological functions of presenilins on a common Ca^{2+} regulatory pathway in both electrically excitable and nonexcitable cells (Grudt et al., 1996; Bouron, 2000). The process of IP_3-mediated Ca^{2+} release from the endoplasmic reticulum (ER) store and replenishing intracellular Ca^{2+} through plasma membrane channels is tightly linked and regulated by the refilling mechanism, termed capacitative calcium entry (CCE) (Putney, 1986, 1990, 1999a; Berridge, 1995; Clapham, 1995). CCE operates through a putative conformation-dependent coupling mechanism between ER Ca^{2+} stores and plasma

§To whom correspondence should be addressed at The Taub Institute for Research on Alzheimer's Disease and the Aging Brain, Columbia University, 630 West 168th Street, P&S 14-511, New York, New York 10032 (e-mail: twk16@columbia.edu).
‖These authors contributed equally to this work.

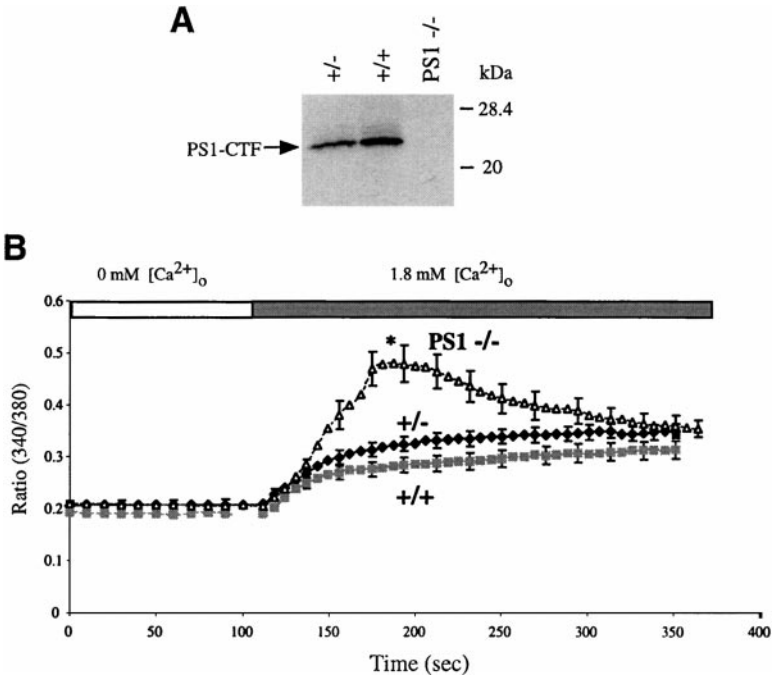

Figure 1. PS1 Deficiency Potentiates the CCE Response

(A) Cultured cortical neurons from day 15.5 embryos from heterozygote (+/−, control 1), homozygote (+/+, control 2), or knockout (−/−) mice were subjected to Western blotting using αPS1Loop antibody.

(B) Potentiation of CCE in PS1-deficient neurons (PS1 −/−) as compared to control 1 (+/−) or control 2 (+/+). Data points are mean fluorescence ratios ± SEM in 27–34 cells (*$p < 0.0001$, compared to controls). CCE was induced by incubating cells with Ca^{2+}-free media containing 2 μM cyclopiazonic acid (CPA) for 30 min and then washing the cells with Ca^{2+}-free HBSS (0 mM $[Ca^{2+}]_o$; see Experimental Procedures) and replacing Ca^{2+}-free buffer with Ca^{2+}-containing media (1.8 mM $[Ca^{2+}]_o$).

membrane CCE channels (Irvine, 1990; Berridge, 1995; Patterson et al., 1999; Yao et al., 1999; Ma et al., 2000).

Here, we show that either elimination of PS1 or expression of inactive PS1 mutants hyperactivates CCE, indicating that functional presenilin is normally required for the proper modulation of CCE. Furthermore, FAD-associated mutations in both PS1 and PS2 universally downregulate CCE in multiple cell types, including neurons. Electrophysiological studies also confirm that CCE channel activity is dramatically diminished by a presenilin FAD mutation. Moreover, we have delineated the temporal order of two separate molecular phenotypes associated with presenilin FAD: Ca^{2+} dyshomeostasis and Aβ42-promoting activity. Our studies indicate that reduced CCE is likely to be an upstream event for the increased generation of Aβ42. Given the putative mechanism of CCE, our studies suggest that the presenilins modulate the coupling between the ER Ca^{2+} stores and the plasma membrane. This activity may be critical for the modulation of CCE and the proteolytic processing of membrane proteins, such as APP.

Results

PS1 Deficiency Enhances CCE Response

Given the previously reported link between PS1 FAD mutations and Ca^{2+} dyshomeostasis, we set out to investigate the possibility that a normal function of PS1 involves the modulation of CCE. To this end, we studied the effects of PS1 deficiency on CCE utilizing cultured primary neurons derived from PS1 knockout mice. Cortical neuronal cultures were prepared from day 15.5 embryos of either heterozygote PS1 +/−, homozygote PS1 +/+, or PS1 −/− mice (Shen et al., 1997). PS1 deficiency in PS1 −/− neurons was verified by Western blot analyses (Figure 1A). To induce CCE artificially, cells were incubated in Ca^{2+}-free media containing an ER Ca^{2+}-depleting reagent, such as cyclopiazonic acid (CPA), and then washed and replenished with Ca^{2+}-containing media (Patterson et al., 1999; Yoo et al., 1999). CCE was then monitored by ratiometric imaging using fura-2/AM (Figure 1B). A dramatic increase in CCE was observed in PS1-deficient neurons as compared to control neurons (Figure 1B); this result indicates that CCE is greatly potentiated by the absence of PS1, suggesting that PS1 may normally be necessary to regulate CCE.

Biologically Active PS1 Is Required for CCE Modulation

To further define the mechanism underlying the enhanced CCE in PS1-deficient neurons, we next examined the effect of abrogation of PS1 biological activities on CCE. For this purpose, we established SY5Y cell lines stably expressing PS1 variant containing a TM aspartate mutation that was shown to abrogate the biological activities of PS1 (D257A-PS1) (Figure 2A). In these cells, the impaired endoproteolytic processing of PS1 resulted in the accumulation of full-length PS1 holoprotein (Wolfe et al., 1999), which largely replaced the endogenous PS1 C-terminal fragment (Figure 2A). We also observed an increased accumulation of putative γ-secretase substrate, the endogenous APP C-terminal fragments (APP-CT83) (Figure 2B), although the increase was not as robust as in a previous study utilizing APP-overexpressing cells (Wolfe et al., 1999; Kimberly et al., 2000). Interestingly, CCE was enhanced by ~125% in D257A-PS1 cells as compared to wild-type PS1 SY5Y cells (Figures 2C and 2D). CCE was also potentiated by two separate TM aspartate mutations (D257A and D385A) in stable CHO cell lines (Figure 2E). These data reveal that mutating the TM aspartate residues, both of which have been shown to abolish the biological activities of PS1, dramat-

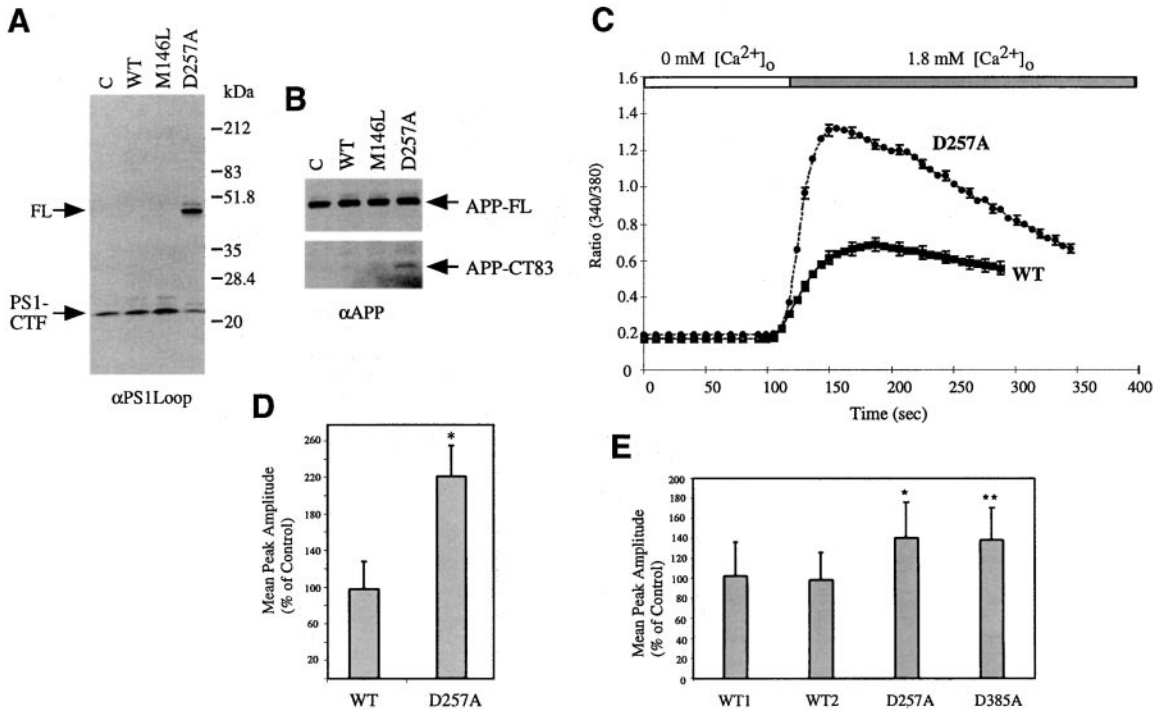

Figure 2. "Loss-of-Function" Transmembrane Aspartate PS1 Mutations Potentiate the CCE Response

(A) Detergent lysates prepared from SY5Y cells stably transfected with vector (C), wild-type PS1 (WT), FAD mutant PS1 (M146L), or D257A-PS1 (D257A) were analyzed by Western blot analyses using αPS1Loop antibody. Arrows denote full-length PS1 (FL) and endoproteolytic PS1 C-terminal fragments (PS1-CTF).

(B) A blot identical to (A) was probed with anti-APP antibody (C7) to detect APP holoprotein (APP-FL) and an endogenous APP C-terminal fragment (APP-CT83).

(C) Potentiation of CCE in SY5Y cells stably expressing D257A-PS1. Data points are mean fluorescence ratios ± SEM in 30 cells.

(D) Mean peak fluorescence amplitudes were calculated from three independent CCE induction experiments using SY5Y cells expressing wild-type PS1 (WT) or D257A-PS1 (D257A). Columns are mean peak amplitudes ± SD, shown as percent of control (*$p < 0.0001$, as compared to WT).

(E) Mean peak fluorescence amplitudes were calculated from two independent CCE induction experiments using four different clonal CHO cell lines expressing wild-type PS1 (WT1 and WT2), D257A-PS1 (D257A), or D385A-PS1 (D385A). Columns are mean peak amplitudes ± SD, shown as percent of control (*$p < 0.0001$, as compared to WT2; **$p < 0.0001$, as compared to WT1).

ically potentiates CCE. These findings indicate that functional PS1 is required for the modulation of CCE.

Effects of Presenilin FAD Mutations on CCE in Stable Transfectants

We next asked whether autosomal dominant presenilin FAD mutations would potentially render any constitutive "gain-of-function" effects on CCE modulation. To examine the effect of a PS1 FAD mutation on CCE, we first utilized SY5Y cells stably transfected with the M146L-PS1 FAD mutant (Figure 2A). When CCE was induced, the amplitude of the CCE response was markedly reduced in the M146L-PS1 cells (~42.5% reduction) as compared to wild-type PS1- or vector-transfected cells (Figures 3A and 3B). In addition to SY5Y cells, CCE was also found to be attenuated in CHO cells stably expressing M146L-PS1 as compared to wild-type PS1 (Figure 3C). To verify that this attenuation of the CCE response was not simply due to the elevated levels of PS protein in our cell lines, we also measured CCE in wild-type or mutant SY5Y cells as well as CHO cells with higher PS expression levels; we found that varying levels of PS protein had no detectable effect on the CCE response (data not shown). Although CCE potentiation by the TM aspartate mutation was much greater in SY5Y cell lines (~125%) as compared to CHO cell lines (~40%) (Figures 2D and 2E), the M146L-PS1 mutation affected CCE to a similar degree in both SY5Y and CHO cells (Figures 3B and 3C).

To determine whether a PS2 FAD mutation would elicit a similar effect on CCE, we established stable SY5Y cell lines expressing either wild-type or the Volga German FAD mutant (N141I) form of PS2 (Figure 3D). In both native and vector-transfected SY5Y cells, PS2 was virtually undetectable in Western blots of straight lysate (Figure 3D; data not shown for native SY5Y cells), indicating that detectable PS2 represents the transgene-derived protein variants in these stable cells. PS2 was detected mainly as endoproteolytic fragments in these cells, while full-length PS2 protein was detectable only after lengthy exposures (Figure 3D). As expected, transgene-derived PS2-CTF "replaced" endogenous PS1-CTF (Figure 3D) (Thinakaran et al., 1997). When CCE was induced, Ca^{2+} influx was dramatically reduced in cells expressing

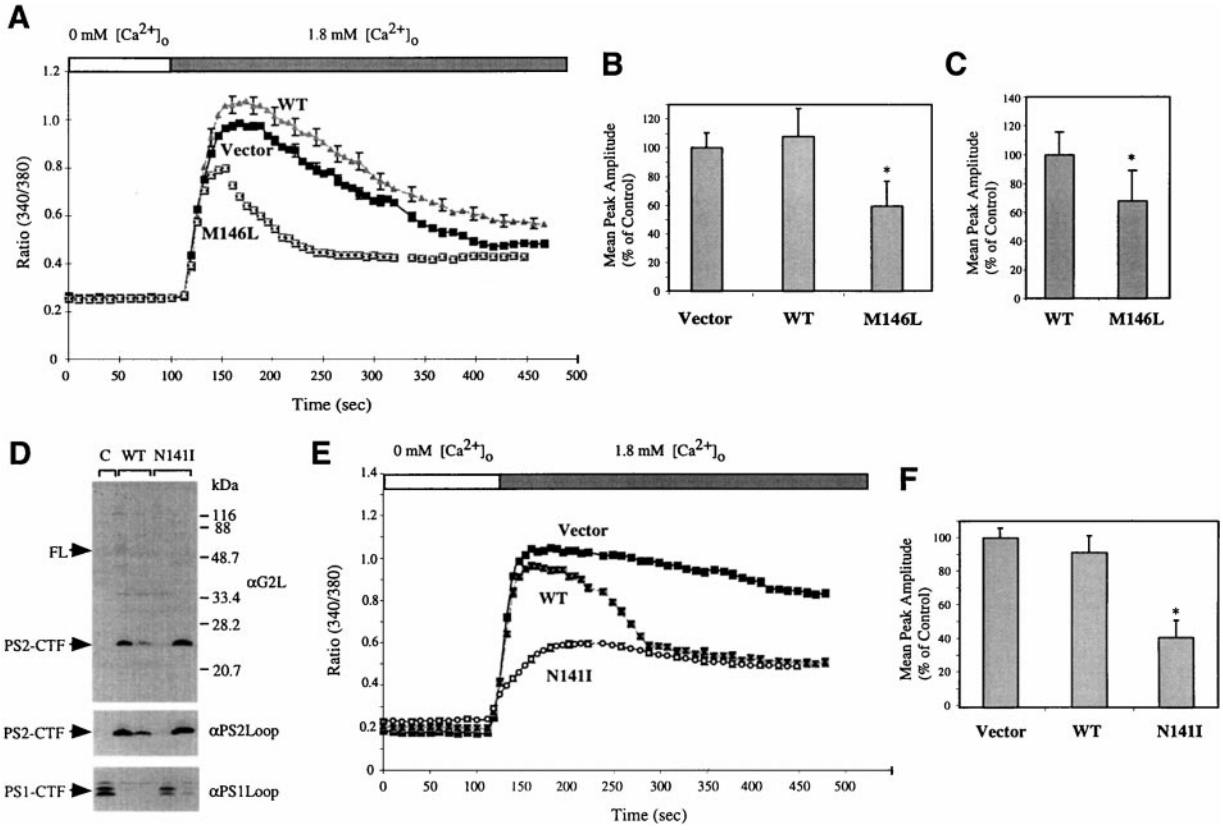

Figure 3. FAD Mutant Presenilins Attenuate CCE

(A) Effect of the M146L PS1 FAD mutation on CCE in stable SY5Y cell lines. CCE was measured by ratiometric imaging in fura-2-loaded SY5Y cells stably transfected with vector, wild-type PS1 (WT), or mutant PS1 (M146L) (n = 26).

(B) Mean peak fluorescence amplitudes were calculated from three independent CCE-induction experiments, using SY5Y cells expressing vector, wild-type PS1 (WT), and mutant PS1 (M146L) (*$p < 0.0001$, compared to WT).

(C) Effect of the M146L PS1 FAD mutation on CCE in stable CHO cell lines. Mean peak fluorescence amplitudes were calculated from four independent CCE induction experiments, using CHO cells stably expressing wild-type PS1 (WT) and mutant PS1 (M146L) (*$p < 0.0001$, compared to WT). In each case, the wild-type and PS1-M146L clonal lines were paired for similar levels of expression.

Data points are mean fluorescence ratios (340 nm/380 nm) ± SEM (A), and columns are mean percent increases ± SD (B and C).

(D) Lysates prepared from stable SY5Y cell lines expressing vector (C) and either wild-type (WT) or FAD mutant (N141I) forms of PS2 were analyzed by Western blotting using the PS2 and PS1 antibodies indicated. Locations of full-length PS2 (FL) and C-terminal fragments of PS2 (PS2-CTF) and PS1 (PS1-CTF) are indicated by arrows.

(E) Effect of the N141I PS2 FAD mutation on CCE in stable SY5Y cell lines. CCE was measured by ratiometric imaging in fura-2-loaded SY5Y cells stably transfected with vector, wild-type PS2 (WT), or mutant PS2 (N141I). Representative data from five independent experiments are shown (n = 33).

(F) Mean peak fluorescence amplitudes were calculated from five separate CCE induction experiments, using SY5Y cells expressing vector, wild-type PS2 (WT), and N141I-PS2 (N141I) (*$p < 0.0001$, compared to WT).

N141I-PS2 as compared to either wild-type PS2 or vector alone (Figure 3E). Multiple experiments were averaged to determine the mean peak amplitudes of CCE. In the N141I-PS2 cells, CCE was reduced by ~58.5% compared to wild-type PS2-transfected cells (Figure 3F). Our results showed that both the M146L PS1 and N141I PS2 mutations carry a gain of function in overregulating CCE.

PS2 FAD Mutation Attenuates CCE in Neurons from Transgenic Mice

We next studied whether FAD mutant presenilin-mediated downregulation of CCE also occurs in neurons. For this purpose, we utilized cultured primary neurons derived from transgenic mice harboring constructs encoding either wild-type or N141I FAD mutant forms of PS2. As a source for these primary neuronal cultures, we generated transgenic mice expressing wild-type or N141I FAD mutant forms of human PS2 under the transcriptional control of the PDGF promoter. The genomic insertion and expression of human PS2 gene was confirmed by genotyping of tail DNA and RT-PCR of mRNA from brain tissues (M. P. F. et al., unpublished data). To assess the expression of human PS2 protein in these transgenic animals, brain extracts of heterozygote animals expressing wild-type or N141I PS2 along with nontransgenic littermates were analyzed by combined immunoprecipitation-Western blot analyses using αP-S2Loop (Figure 4A). Elevated levels of PS2-CTF were observed in groups of transgenic mice expressing hu-

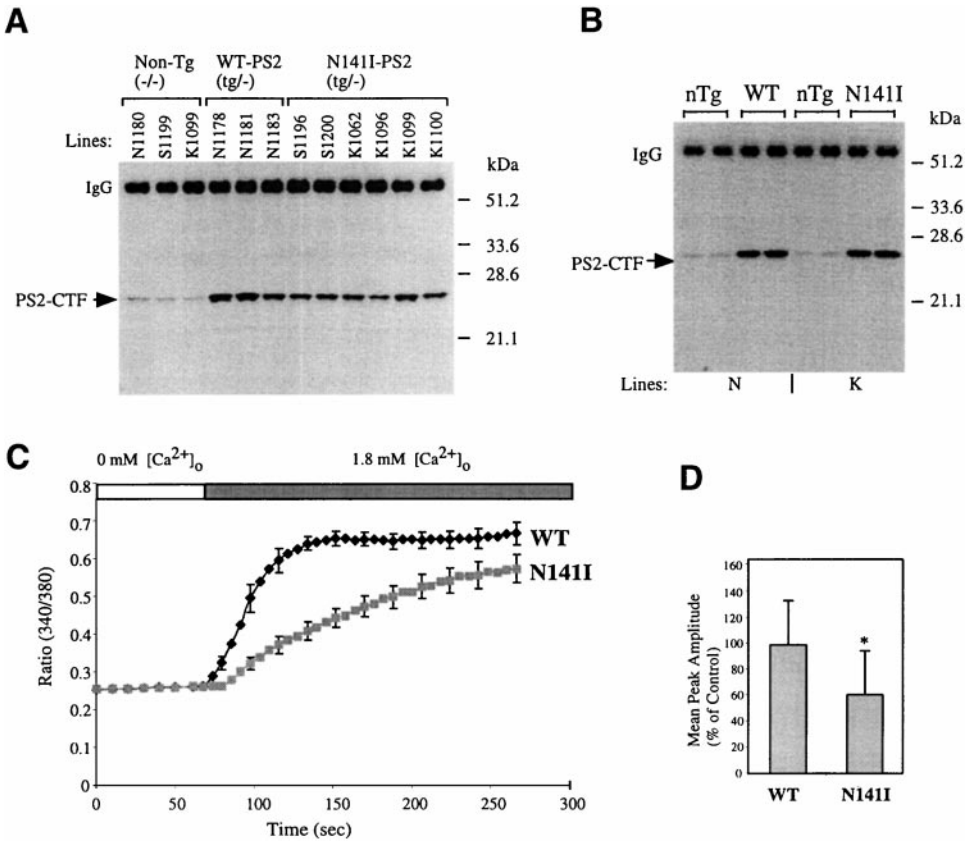

Figure 4. Primary Cortical Neurons Derived from N141I-PS2 Transgenic Mice Exhibit Attenuated CCE

(A) Characterization of PS2 in transgenic mice. Immunoprecipitation–Western blotting analysis was performed using αPS2Loop in the lysates prepared from brain tissues of transgenic mice expressing a construct encoding either wild-type (WT-PS2) or N141I FAD mutant (N141I-PS2) PS2, along with nontransgenic samples (Non-Tg).

(B) Lines with similar levels of protein expression were paired among N and K lines, and protein extracts were analyzed by immunoprecipitation–Western blotting analysis. A representative blot is shown.

(C) Effects of the N141I-PS2 mutation on CCE in cultured cortical neurons from day 18.5 embryos.

(D) Average mean peak amplitudes were shown as mean fluorescence ratios (340 nm/380 nm) ± SD ($n = \sim 50$; *$p < 0.0001$, compared to WT).

man wild-type PS2 and N141I-PS2 transgenes (Figure 4A). In all PS2 founder transgenic mouse lines selected for the test, no detectable full-length PS2 polypeptides were observed (data not shown). Founder lines with similar expression levels of PS2-CTF were selected for breeding and further use (Figure 4B).

Cortical neuronal cultures were prepared from day 18.5 embryos of either heterozygote wild-type or N141I mutant PS2 animals. Embryos were plated in separate chambers, and corresponding tissues were removed from each embryo and used for genotyping. In the neuronal cultures, nonneuronal cells were less than ~10% (data not shown), and cell bodies of morphologically differentiated neurons were selected to conduct Ca^{2+} imaging experiments ($n = \sim 50$). CCE was dramatically suppressed in N141I-PS2 neurons as compared to wild-type PS2 neurons (Figure 4C). Three independent Ca^{2+} imaging experiments were performed to determine mean peak amplitudes, indicating a ~50% reduction of CCE in N141I-PS2 neurons as compared to wild-type PS2 neurons (Figure 4D). Similar to what was observed in SY5Y cells, the amplitudes of CCE in neurons of wild-type animals were similar to those in neurons from nontransgenic animals (data not shown).

CCE Inhibitors, but Not L- or N-Type Ca^{2+} Channel Antagonists or Cytochalasin D, Abolish the Effects of FAD Mutant Presenilin on CCE

To further characterize Ca^{2+} influx pathway(s) affected by presenilin FAD mutations, we studied the effects of various pharmacological reagents on CCE. The Ca^{2+} influx observed in all cell lines was blocked by pretreatment with the CCE inhibitors SKF96365 (Merritt et al., 1990; Mason et al., 1993) and Calyculin A (CalyA) (Patterson et al., 1999; Ma et al., 2000) (Figures 5A and 5C). However, nifedipine and ω-conotoxin GVIA, which inhibit L- and N-type Ca^{2+} channels, respectively, had virtually no effect on Ca^{2+} influx (Figures 5B and 5C). Thus, the alterations in $[Ca^{2+}]_i$ were likely CCE specific. In addition, the CCE reduction in M146L cells was unaffected by the presence of nifedipine and ω-conotoxin GVIA (data not shown), suggesting that the mechanism underlying reduced CCE in mutant cells is independent of these types of voltage-operated Ca^{2+} channels. To ensure that

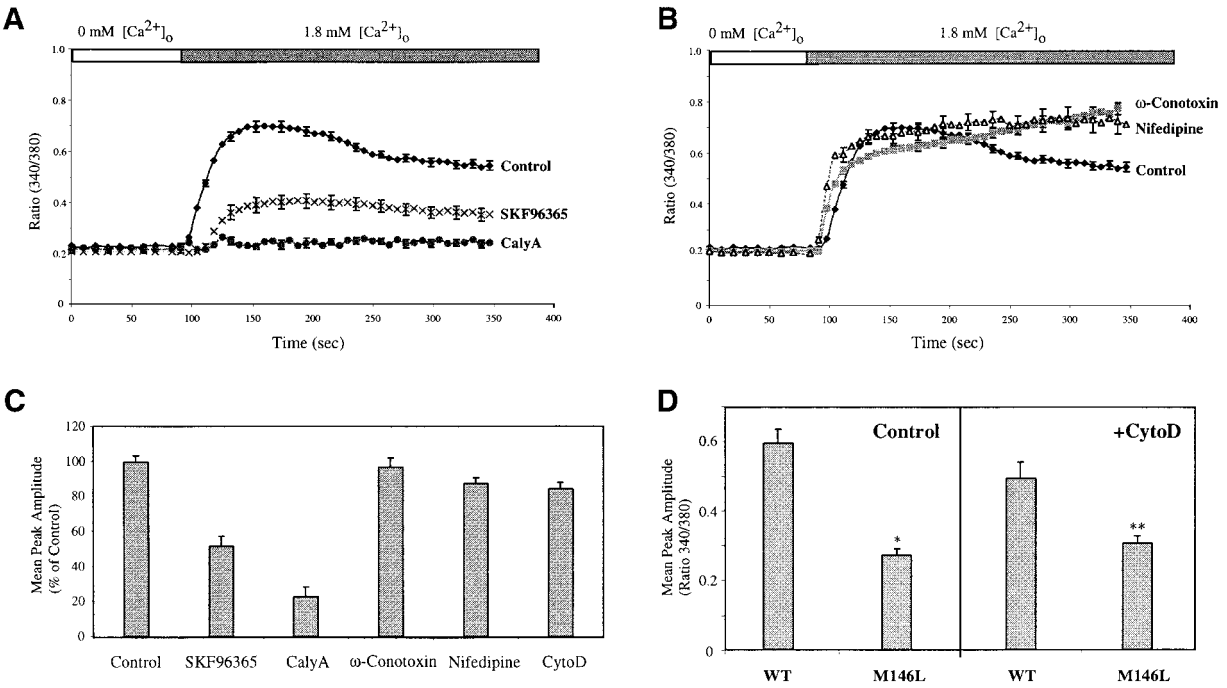

Figure 5. CCE-Specific Properties of the Observed Ca^{2+} Influx in SY5Y Cell Lines

(A) Inhibition of CCE by SKF96365 or CalyA. SY5Y cells stably expressing wild-type PS2 were pretreated with either 100 μM SKF96365 for 1 hr or 100 nM CalyA for 20 min prior to induction of CCE.

(B) Effects of L-type or N-type voltage-operated Ca^{2+} channel antagonists nifedipine (1 μM) and ω-conotoxin GVIA (2 μM), respectively, on the CCE response in SY5Y cells.

(C) Relative effects of SKF96365, CalyA, ω-conotoxin GVIA, nifedipine, and CytoD on CCE in wild-type PS2 cells. Columns are mean peak amplitudes ± SD, shown as percent of control.

(D) CytoD has no effect on the observed reduction in CCE caused by the M146L PS1 mutation. Mean peak amplitudes were determined from three independent experiments using SY5Y cells expressing wild-type PS1 (WT) or mutant PS1 (M146L), either without (Control) or with (+CytoD) a 2 hr pretreatment of 2 μM CytoD. Columns are mean peak amplitudes in fluorescence ratios ± SD (*$p < 0.0001$ and **$p < 0.001$, respectively, as compared to WT).

the FAD mutations were actually affecting CCE and not other types of Ca^{2+} influx, we tested additional previously reported properties of CCE. One of the key features of CCE is its lack of requirement for intact actin cytoskeleton. For instance, disruption of the intracellular cytoskeleton by treatment with Cytochalasin D (CytoD) impairs the IP_3-elicited release of Ca^{2+} from internal stores (Ribeiro et al., 1997); in contrast, CytoD has no effect on CCE (Ribeiro et al., 1997; Patterson et al., 1999). We examined whether CytoD could abolish the effect of PS FAD mutations on Ca^{2+} influx (Figures 5C and 5D). CytoD had essentially no effect on Ca^{2+} influx in either wild-type PS1 or M146L-PS1 cells and had no effect on the reduced CCE phenotype seen in M146L-PS1 cells (Figure 5D). Similar results were found using N141I-PS2 cells (data not shown). FAD-associated presenilin mutations may therefore affect CCE directly and independent of the Ca^{2+} mobilization pathways that require an intact cytoskeleton.

Impaired I_{CRAC} in M146L-PS1 Cells

Functional activities of putative plasma membrane CCE channels can be detected as calcium release–activated Ca^{2+} current, also known as store-operated Ca^{2+} current (I_{CRAC}) (Hoth and Penner, 1992; Zweifach and Lewis, 1993). The effects of presenilin FAD mutations on CCE were further investigated by examining I_{CRAC} in wild-type and M146L-PS1 CHO cells (Figure 6). The time course of activation of I_{CRAC} was determined in single cells followed by passive store depletion via patch pipettes containing Ca^{2+}-chelating reagent BAPTA in the whole-cell configuration, and Na^{2+} was used as the charge carrier (Kerschbaum and Cahalan, 1999). The currents were activated slowly under this condition and reached the maximal level in ~5 min in the wild-type PS1 cells after establishment of the whole-cell configuration (Figures 6A and 6B). In contrast, M146L-PS1 cells exhibited severely impaired I_{CRAC} (Figures 6A and 6B). Similar data have been obtained using stable M146L-PS1 SY5Y cell lines (data not shown). The average current density was significantly reduced in M146L-PS1 CHO cells as compared to wild-type cells (Figure 6C). Under our experimental conditions, pretreatment of cells with SKF96365 virtually eliminated I_{CRAC} in wild-type PS1 CHO cells (Figure 6C), indicating that I_{CRAC} is sensitive to pretreating cells with SKF96365.

A novel arachidonate-regulated current (I_{ARC}) has been reported, and channel properties of I_{ARC} appeared to be similar to that of I_{CRAC} (Shuttleworth, 1996). However, I_{ARC} is activated even after the store depletion (Mignen and Shuttleworth, 2000). We tested whether PS1 FAD mutation affects I_{ARC} after the induction of I_{CRAC} via store deple-

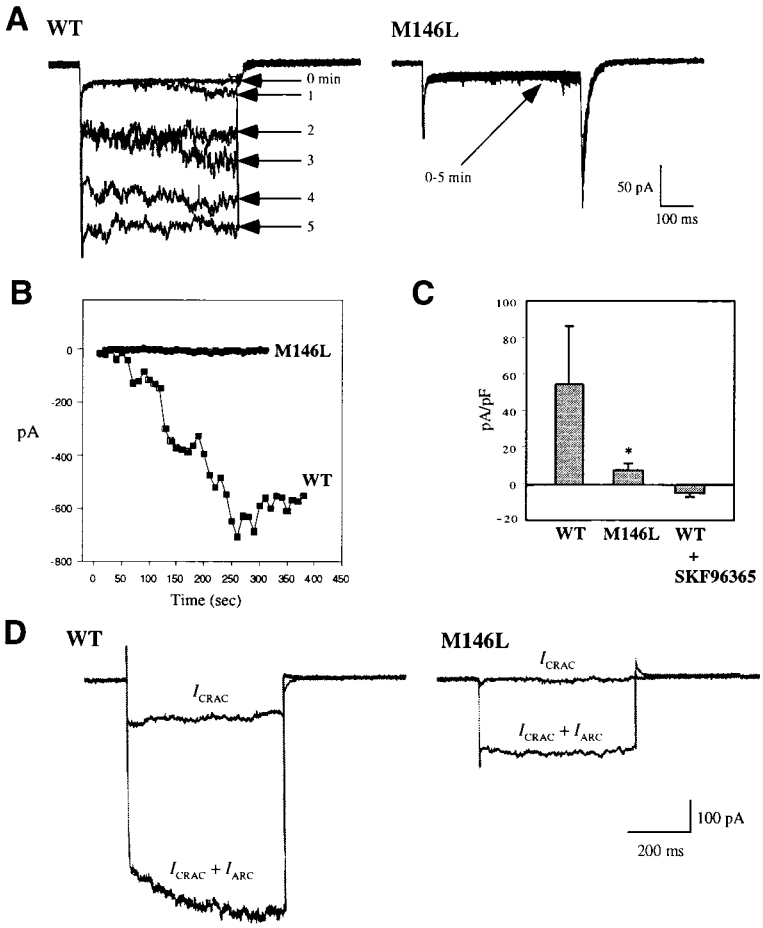

Figure 6. Impaired Calcium Release–Activated Calcium Currents (I_{CRAC}) in M146L-PS1 Cells

(A) I_{CRAC} channel activities were measured in the stable CHO cells expressing either wild-type (WT) or FAD mutant (M146L) PS1 by the whole-cell patch clamp experiments. The currents were activated following dialysis with 10 mM BAPTA (passive depletion). Membrane potential was held at 0 mV, and hyperpolarizing voltage pulses at −120 mV were applied every 10 s. The transient and leak currents were not canceled.

(B) Comparison of time courses of the activation of I_{CRAC} channels in wild-type and M146L PS1 cells. Inward currents were evoked by applying hyperpolarizing pulse at 120 mV at a holding potential of 0 mV. Data points are the current levels measured every 10 s. The leak currents were canceled.

(C) Comparison of average peak I_{CRAC} current densities (pA/pF) from wild-type (WT) and M146L-PS1 cells. Wild-type PS1 cells were also pretreated in parallel with 10 μM SKF96365 for 30 min before the current measurement (WT + SKF96365). The average peak current density in M1465L-PS1 cells was significantly smaller than that of wild-type PS1 cells ($n = 23$, $^*p < 0.05$).

(D) Arachidonate-regulated Ca^{2+} currents (I_{ARC}) were preserved in M146L-PS1 cells. After I_{CRAC} currents reached the stable levels in 6–7 min, arachidonic acid (8 μM) was added to induce I_{ARC} currents on top of I_{CRAC} currents. Currents were measured as described in (A).

tion. Arachidonic acid–induced currents followed by I_{CRAC} were preserved in both wild-type and M146L-PS1 cells (Figure 6D). This indicates that presenilin FAD specifically affects the store-dependent current I_{CRAC} but not store-independent currents such as I_{ARC}.

A CCE Inhibitor, SKF96365, Elevates Aβ42 Levels

To gain insight into the molecular link between the PS FAD-driven changes in the CCE response and alterations in Aβ42 production, we first examined the effect of the CCE antagonist SKF96365 on Aβ production using a sensitive Aβ-specific sandwich ELISA (Johnson-Wood et al., 1997; Xia et al., 1997). SKF96365 decreased both store depletion–activated Ca^{2+} influx (Figure 5A) and currents (Figure 6C). Since Aβ levels (e.g., Aβ42) in SY5Y cells are not readily detectable, we utilized CHO or 293 cells stably overproducing human APP695. SKF96365 has been shown to have a minor inhibitory effect on voltage-operated Ca^{2+} channels (Merritt et al., 1990; Mason et al., 1993; Grudt et al., 1996); therefore, we included nifedipine and ω-conotoxin GVIA as negative controls to ensure the CCE specificity of SKF96365 on Aβ generation. The concentrations of SKF96365, nifedipine, and ω-conotoxin GVIA were chosen based on the previous studies (Grudt et al., 1996; Vazquez et al., 1998; Jayadev et al., 1999). Interestingly, treatment of CHO or 293 cells stably overexpressing human APP with SKF96365 specifically elevated the ratio of Aβ42/Aβtotal (Figures 7A and 7B). In contrast, nifedipine and ω-conotoxin GVIA had no significant effect on Aβ42 generation (Figures 7A and 7B). This Aβ42-promoting effect of SKF96365 was dose dependent (Figure 7C) and inversely correlated with relative magnitudes of CCE (Figure 7D). Under these conditions, SKF96365 treatment did not alter secreted APP-α levels or cell viability in these cultures (data not shown). Thus, inhibition of the cellular pathways involving CCE specifically increases Aβ42, which is a molecular phenotype linked to FAD mutant presenilins.

Aβ42-Promoting Effect of SKF96365 Requires Biological Activity of Presenilins

We next tested whether the Aβ42-elevating effect of SKF96365 requires the biological activity of the presenilins. For this purpose, we treated CHO cells stably expressing D257A-PS1 with SKF96365 and measured Aβ generation. As previously reported (Wolfe et al., 1999), total Aβ levels were dramatically lower in D257A-PS1 cells than in wild-type PS1-expressing CHO cells (Figure 7E). Aβ42 was also reduced in D257A-PS1 cells relative to wild-type PS1 cells, but to a lesser extent than total Aβ (Figure 7F). Treatment with SKF96365 did not restore the generation of either total Aβ or Aβ42 in the D257A-PS1 cells, indicating that the biological activity of PS1 is required for the Aβ42-promoting effect of SKF96365. In D257A cells, relative Aβ42 levels follow-

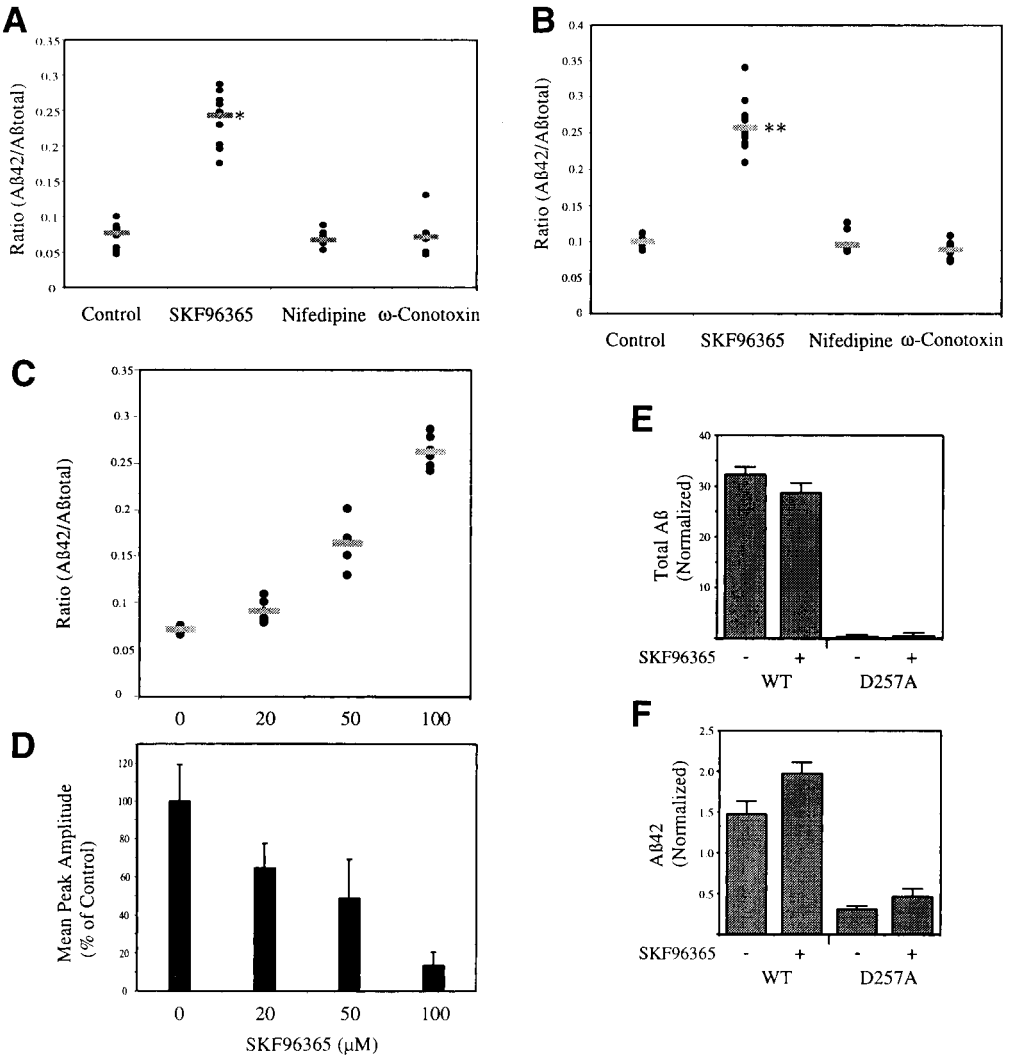

Figure 7. Effects of a CCE Inhibitor, SKF96365, on Aβ Generation

(A and B) Effects of SKF96365 (100 μM), nifedipine (1 μM), and ω-conotoxin GVIA (1 μM) on the ratio of Aβ42/Aβtotal in CHO (A) or HEK293 (B) cells stably overexpressing human APP (12 hr treatment). Controls were DMSO (solvent) only. Amounts of Aβ42 and Aβtotal were determined by sandwich ELISA. The ratios of Aβ42/Aβtotal from three independent experiments are plotted. Horizontal bars represent average Aβ42 to Aβtotal ratios ($n = 12$, *$p < 0.0001$ and **$p < 0.0005$, respectively, as compared to controls).

(C and D) Correlation of reduced CCE and increases in the Aβ42/Aβtotal ratio. CHO cells stably expressing human APP were treated with indicated concentrations of SKF9635 for 12 hr. Relative mean peak amplitudes (D) and corresponding Aβ42/Aβtotal ratios (C) are shown.

(E and F) CHO cells stably expressing APP and PS1 variants (either PS1 wild-type [WT] or D257A-PS1 [D257A]) were incubated in the absence (−) or presence (+) of 50 μM SKF96365. Columns represents relative amounts of total Aβ (E) or Aβ42 (F) in the culture media. All values were normalized to total protein amounts in the cell lysates.

ing treatment with SKF96365 was greater than 90% of total Aβ levels (Figures 7E and 7F). Under identical conditions (50 μM SKF96365, 12 hr), the degree of CCE reduction in D257A-PS1 cells was much less compared to wild-type PS1 cells' reduction (data not shown).

Elevated APP or Aβ42 Do Not Alter CCE

We next tested whether CCE reduction by FAD-linked presenilin mutations might be due to the increased accumulation of Aβ42. Utilizing CHO-APP cells that produce substantially elevated levels of APP and Aβ42 (Xia et al., 1997), we found that stable overproduction of APP (and the subsequent increase in Aβ42) had virtually no effect on CCE (Figure 8A). Furthermore, pretreatment of the cells with Aβ42 also had no detectable effect on the CCE response (Figure 8A versus Figure 8B). Cell viability was not affected under these conditions, and similar data have been obtained using 293 and SY5Y cell lines (data not shown). Therefore, the reduced CCE in FAD mutant presenilin cells is not likely to be due to increased extracellular or intracellular levels of Aβ42.

Discussion

The presence of biologically active PS1 or PS2 is essential for the generation of Aβ through γ-secretase cleav-

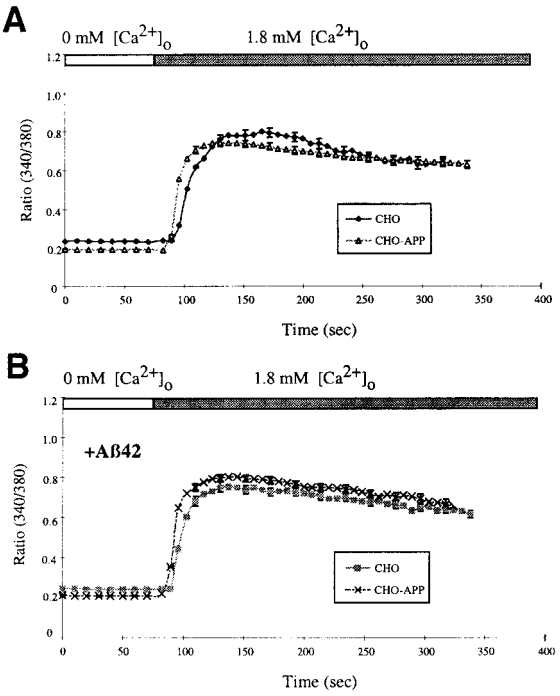

Figure 8. Elevated APP or Aβ42 Levels Confer No Effects on CCE

Effect of stable overexpression of human APP (A) and Aβ42 pretreatment (B) on the CCE response in CHO cells.

(A) CCE was assayed by ratiometric Ca^{2+} imaging using either native CHO cells (CHO) or CHO cells stably overexpressing human APP_{695} (CHO-APP).

(B) CHO and CHO-APP cells were preincubated with 20 μM Aβ42 for 3 hr prior to induction of CCE (compare to [A]). Data points are mean fluorescence ratios ± SEM in 33 cells.

age of APP (De Strooper et al., 1998). Our current studies demonstrated that abrogation of biological activities of PS1, by either knocking out PS1 or expressing inactive PS1 mutants, greatly potentiated CCE, suggesting that a normal function of PS1 (and perhaps PS2) is to modulate CCE. We also showed that treating cells with a CCE inhibitor (SKF96365) downregulates CCE and I_{CRAC} and selectively elevates Aβ42 generation. However, increased cellular levels of Aβ42 had no effect on CCE, suggesting that reduced CCE might be an early cellular event leading to the increased Aβ42 generation associated with presenilin FAD mutations. Interestingly, preliminary data revealed that direct inhibition of Aβ generation using a synthetic γ-secretase inhibitor displayed no effects on CCE, further supporting the idea that presenilin-mediated modulation of CCE is an upstream event of Aβ generation (T.-W. K., unpublished data).

According to our model, autosomal dominant FAD mutant presenilins exert a gain of function by downregulating CCE while increasing IP_3-mediated release from the ER store, leading to diminished luminal Ca^{2+} concentration ($[Ca^{2+}]_{ER}$) (Waldron et al., 1997; Hofer et al., 1998). It is interesting to note that changes in $[Ca^{2+}]_{ER}$ influence a number of cellular functions, including chaperone activities and gene expression (reviewed by Meldolesi and Pozzan, 1998). Therefore, it is tempting to speculate that reduced CCE may also be an upstream event leading to other molecular phenotypes associated with FAD mutant presenilins, including altered unfolded protein response (Katayama et al., 1999; Niwa et al., 1999) and increased vulnerability to apoptotic stimuli (Deng et al., 1996; Wolozin et al., 1996; Janicki and Monteiro, 1997). Interestingly, in transgenic mice harboring spinocerebellar ataxia type 1 (SCA1) mutant gene products, TRP3, SERCA2, and IP_3-R, all components of CCE, were specifically downregulated. This suggests the potential contribution of CCE dysregulation in other neurodegenerative diseases in addition to AD (Lin et al., 2000). CCE involves direct physical interaction between the ER and plasma membrane constituents (reviewed by Putney, 1999a; Berridge et al., 2000). According to this conformational coupling mechanism, a conformational change of the IP_3 receptor (IP_3-R) upon agonist stimulation and subsequent release of Ca^{2+} leads to the formation of a molecular complex containing IP_3-R bound to molecular constituents in the plasma membrane harboring CCE channels. This then allows extracellular Ca^{2+} to replenish the ER store (Kiselyov et al., 1998, 1999; Boulay et al., 1999; Putney, 1999a). It has been postulated that the presenilins modulate the γ-secretase activity via few possible mechanisms: the presenilins might be the γ-secretases themselves, serve as essential cofactors for the γ-secretase action, or regulate intracellular trafficking of a putative γ-secretase to the target site where relevant substrates are localized (De Strooper et al., 1998; Naruse et al., 1998; Wolfe et al., 1999; reviewed by Selkoe, 2000). Given a role for presenilins in governing CCE, the presenilins may also modulate proteolytic processing of APP and Notch at or near the cell surface (Annaert and De Strooper, 1999) at sites of ER–plasma membrane coupling. It is conceivable that the presenilins may regulate or directly mediate the cleavage of protein(s) involved in modulating CCE. In any event, a gain in the biological activity of the presenilins, owing to autosomal dominant FAD mutations, may attenuate CCE while increasing γ-secretase activity. Further experimentation will be necessary to elucidate this connection. Finally, augmentation of CCE, through the identification of agonists of plasma membrane store–operated Ca^{2+} channels (e.g., TRP or as yet undiscovered CCE channels) that mediate CCE (Birnbaumer et al., 1996; Zhu et al., 1996; Li et al., 1999; Putney, 1999b; Philipp et al., 2000), could potentially be employed to reduce PS-associated γ-secretase activity, and the generation of Aβ as a novel therapeutic means for preventing or treating AD.

Experimental Procedures

Cell Culture, Generation of Stable Cell Lines, and Aβ Treatment

Stable PS1 SY5Y cell lines were generated by transfecting 0.5 μg of pBabe along with 5 μg of each plasmid: PS1, M146L-PS1, D257A-PS1, or vector alone (pcDNA3.1) using Superfect transfection reagent (Qiagen). Individual puromycin-resistant colonies were isolated and screened for PS1 expression by Western blotting. Stable PS1 SY5Y cell lines were maintained in DMEM supplemented with 10% fetal calf serum and penicillin/streptomycin in the presence of 1 μg/ml puromycin (Sigma) at 37°C in 5% CO_2 incubator. Other stable cell lines, including PS2 SY5Y cells (Pack-Chung et al., 2000) and PS1 CHO cells (Wolfe et al., 1999), have previously been described. The Aβ42 peptides were obtained from Bachem and dissolved in PBS at 1 mg/ml directly before use.

Western Blot Analysis and Immunoprecipitation

Western blot and immunoprecipitation analyses were performed as previously described (Pack-Chung et al., 2000). Brain tissues from the transgenic animals were homogenized in solution A (0.32 M sucrose, 1 mM $MgCl_2$, 0.5 mM $CaCl_2$, 1 mM $NaHCO_3$) containing protease inhibitors using a motor-operated Teflon glass homogenizer. The resulting tissue homogenate was lysed using IP buffer (10 mM Tris-HCl [pH 7.4], 150 mM NaCl, 1% Triton X-100, 0.25% NP-40, 2 mM EDTA) and subjected to immunoprecipitation, SDS–PAGE, and Western blot analysis. To detect secreted APP produced from the α-secretase-mediated cleavage of APP (APPs-α), media collected from the abovementioned samples of 293 cells were immunoprecipitated by antibody 22C11 and blotted with antibody 6E10.

Calcium Imaging

Briefly, cells are grown on 25 mm round glass coverslips for at least 24 hr before measuring $[Ca^{2+}]_i$. Fura-2 acetoxymethyl ester (fura-2/AM) is dissolved in DMSO and further solubilized in Pluronic acid (0.08%), in HBSS (145 mM NaCl, 2.5 mM KCl, 1 mM $MgCl_2$, 20 mM HEPES, 10 mM glucose, and 1.8 mM $CaCl_2$) containing BSA (1%). When Ca^{2+}-free medium is used, Ca^{2+} is replaced with 50 μM EGTA. Fura-2/AM is loaded into cells by incubation with HBSS containing fura-2/AM (5 μM) at 37°C for 30 min. Fluorescence emission at 505 nm is monitored at 25°C using a dual wavelength spectrofluorometer system with excitation at 340 and 380 nm. Ratios (fluorescence intensity at 340 nm/380 nm) are obtained from 8-frame averages of pixel intensities at each of the excitation wavelengths. Statistical analyses were performed by two-tailed unpaired t test using InStat software.

Electrophysiology

Patch clamp experiments were conducted in the whole-cell configuration using Axopatch 200B amplifier and digidata 1200 interface. The pipettes were fire polished and had a final resistance of 3–4 MΩ. To obtain whole-cell configuration, cell attached patches were formed, and the cell membrane under the patch pipette was ruptured by gentle suction. Currents were sampled at 5 kHz and digitally filtered at 500 Hz. Data acquisition and analysis were performed using pClamp 6.0. All experiments were done at room temperature (20–23°C). Initial traces obtained on going whole-cell were averaged and averaged for leak subtraction. Data analysis was performed by using the Students t test. A difference was considered statistically significant when $p < 0.05$. All results are given as means $\pm$ SEM. Divalent cation-free external solution contained 150 mM Na^+ methane sulfonate, 10 mM *N*-hydroxyethyl-ethylenediamine-triacetic acid (HEDTA), and 10 mM HEPES (pH 7.2). In some experiments, external solution containing 20 mM $CaCl_2$ in addition to 120 mM Na^+ methane sulfonate was used. The pipette solution contained 128 mM Na^+-Aspartate, 10 mM HEPES, 12 mM 1,2-bis(2-aminophenoxy)ethane-*N,N,N*=,*N*=-tetraacetic acid (BAPTA), 0.9 mM $CaCl_2$, and NaOH (pH 7.2).

Generation of Human PS2 Transgenic Mice

To construct the transgene vector, the CMV promoter was excised from the expression vector pCI (Promega) and replaced with an oligonucleotide polylinker into which the PDGF B chain promoter fragment was inserted. The wild-type and N141I mutant PS2 cDNAs in the pcDNA3.1-Zeo(+) backbone were subcloned into the pCI vector containing PDGF B chain promoter. DNA fragments containing PS2 transgenes were microinjected into pronuclei of fertilized mouse zygotes in the Transgenic Mouse Core Facility (Department of Pathology, Brigham and Women's Hospital, Boston, MA). Mice expressing either wild-type or N141I mutant form of PS2 were generated and genotyped using tail-extracted DNAs. Transgene expression was confirmed by RT–PCR using a human PS2-specific primer set. Expression of human PS2 protein was confirmed using combined immunoprecipitation–Western blot analyses.

Primary Cortical Neuronal Cultures

Briefly, pregnant mice are sacrificed on E15.5 (E18.5 for culturing primary neurons from PS2 transgenic mice). The morning of the day the vaginal plugs are observed is designated as E0.5. The uterus is removed under sterile conditions and the embryos are rapidly transferred to HBSS dissociation media. The dissociation media contains 1× HBSS (Gibco, Grand Island, NY), 15 mM HEPES, 7.5% sodium bicarbonate, and 2.47 g/0.5 L glucose (pH 7.4). The tails are harvested for DNA extraction and PCR analysis of genotype. The brain is dissected out of the head with forceps, and the pia and connective tissue are carefully removed. After dissection is complete, brains are washed with fresh HBSS dissociation media, and the tissue is transferred to a 15 ml falcon tube containing 1 ml trypsin and 0.001% DNase. Tubes are placed in a 37°C water bath for 10–12 min and are shaken every 2–3 min to break the clump of tissues. Neurobasal media (1.5 ml) with 10% serum is added to each of the tubes. Cell are mildly dissociated using a polished Pasteur pipette. Tissues are allowed to settle at room temperature for 4–6 min. The supernatant is removed and spun for 5 min at room temperature at 1000 rpm, and pellets are resuspended in 2 ml neurobasal media with serum. Cells are counted and plated at a density of 40,000 cells/cm^2. Cells are plated onto 25 mm coverslips coated with poly-L-lysine (0.25 mg/ml). After 2 hr, media are removed and replaced with neurobasal media supplemented with B27, glutamine, and Pen/Strep.

Quantitation of Aβ Using Sandwich ELISA

Aβ sandwich ELISA was performed as previously described (Johnson-Wood et al., 1997). Ab266 (to Aβ residues 13–28) and 21F12 (to Aβ residues 33–42) were used as capture antibodies for Aβtotal and Aβ42, respectively. Biotinylated 3D6 (to Aβ residues 1–5) was used as the reporter antibody for both Aβtotal and Aβ42 assays.

Acknowledgments

We thank T. Rahmati and D. J. Selkoe for Aβ ELISAs, M. Wolfe for the D257A-PS1 construct, K. T. Kim for helpful discussions, G. E. Gibson for critical comments on the manuscript, and T. Tomita, T. Iwatsubo, G. Thinakaran, and S. Sisodia for antibodies. This work was supported by the National Institute on Aging grants AG18026 (T.-W. K.), AG05845 (A. J. S.), and AG15379 (R .E. T.) and grants from the American Health Assistance Foundation (T.-W. K.), Alzheimer's Association (R. E. T.), Partners Healthcare System (T.-W. K.), and Brain Science and Engineering Research Program sponsored by the Korean Ministry of Science and Technology (S. C.). I. C. is a Howard Hughes Medical Institute Medical Student Training Fellow and T.-W. K. is a recipient of the Partners Investigator (Nesson) Award.

Received May 23, 2000; revised July 6, 2000.

References

Annaert, W., and De Strooper, B. (1999). Presenilins: molecular switches between proteolysis and signal transduction. Trends Neurosci. *22,* 439–443.

Berridge, M.J. (1995). Capacitative calcium entry. Biochem. J. *312,* 1–11.

Berridge, M.J., Lipp, P., and Bootman, M.D. (2000). The calcium entry pas de deux. Science *287,* 1604–1605.

Birnbaumer, L., Zhu, X., Jiang, M., Boulay, G., Peyton, M., Vannier, B., Brown, D., Platano, D., Sadeghi, H., Stefani, E., and Birnbaumer, M. (1996). On the molecular basis and regulation of cellular capacitative calcium entry: roles for Trp proteins. Proc. Natl. Acad. Sci. USA *93*, 15195–15202.

Borchelt, D.R., Thinakaran, G., Eckman, C.B., Lee, M.K., Davenport, F., Ratovitsky, T., Prada, C.-H., Kim, G., Seekins, S., Yager, D., et al. (1996). Familial Alzheimer's disease-linked presenilin 1 variants elevate Aβ1-42/1-40 ratio in vitro and in vivo. Neuron *17,* 1005–1013.

Boulay, G., Brown, D.M., Qin, N., Jiang, M., Dietrich, A., Zhu, M.X., Chen, Z., Birnbaumer, M., Mikoshiba, K., and Birnbaumer, L. (1999). Modulation of Ca^{2+} entry by polypeptides of the inositol 1,4,5-triphosphate receptor (IP3R) that bind transient receptor potential (TRP): evidence for roles of TRP and IP3R in store-depletion activated Ca^{2+} entry. Proc. Natl. Acad. Sci. USA *96,* 14955–14960.

Bouron, A. (2000). Activation of a capacitative Ca^{2+} entry pathway

by store depletion in cultured hippocampal neurons. FEBS Lett. *470,* 269–272.

Capell, A., Grünberg, J., Pesold, B., Diehlmann, A., Citron, M., Nixon, R., Beyreuther, K., Selkoe, D.J., and Haass, C. (1998). The proteolytic fragments of the Alzheimer's disease-associated presenilin 1 form heterodimers and occur as a 100-150 kDa molecular mass complex. J. Biol. Chem. *273,* 3205–3211.

Citron, M., Westaway, D., Xia, W., Carlson, G., Diehl, T., Levsque, G., Johnson-Wood, K., Lee, M., Seubert, P., Davis, A., et al. (1996). Mutant presenilins of Alzheimer's disease increase production of 42-residue amyloid β-protein in both transfected cells and transgenic mice. Nat. Med. *3,* 67–72.

Clapham, D.E. (1995). Calcium signaling. Cell *80,* 259–268.

Cook, D.G., Sung, J.C., Golde, T.E., Felsenstein, K.M., Wojczk, B.S., Tanzi, R.E., Trojanowski, J.Q., Lee, V.M.-Y., and Doms, R.W. (1996). Expression and analysis of presenilin 1 in a human neuronal system: localization in cell bodies and dendrites. Proc. Natl. Acad. Sci. USA *93,* 9223–9228.

Deng, G., Pike, C.J., and Cotman, C.W. (1996). Alzheimer-associated presenilin-2 confers increased sensitivity to apoptosis in PC12 cells. FEBS Lett. *397,* 50–54.

De Strooper, B., Saftig, P., Craessaerts, K., Vandersticheles, H., Guhde, G., Annaert, W., Von Figura, K., and Van Leuven, F. (1998). Deficiency of presenilin-1 inhibits the normal cleavage of amyloid precursor protein. Nature *391,* 387–390.

De Strooper, B., Annaert, W., Cupers, P., Safig, P., Craessaerts, K., Mumm, J.S., Schroeter, E.H., Schrijvers, V., Wolfe, M.S., Ray, W.J., et al. (1999). A presenilin-1-dependent γ-secretase-like protease mediates release of Notch intracellular domain. Nature *398,* 518–522.

Doan, A., Thinakaran, G., Borchelt, D.R., Slunt, H.H., Ratovitsky, T., Podlisny, M., Selkoe, D.J., Seeger, M., Gandy, S.E., Price, D.L., and Sisodia, S.S. (1996). Protein topology of presenilin 1. Neuron *17,* 1023–1030.

Duff, K., Eckman, C., Zehr, C., Yu, X., Prada, C.-M., Perez-Tur, J., Hutton, M., Buee, L., Harigaya, Y., Yager, D., et al. (1996). Increased amyloid-β42(43) in brains of mice expressing mutant presenilin 1. Nature *383,* 710–713.

Etcheberrigaray, R., Hirashima, N., Nee, L., Prince, J., Govoni, S., Racchi, M., Tanzi, R.E., and Alkon, D.L. (1998). Calcium responses in fibroblasts from asymptomatic members of Alzheimer's disease families. Neurobiol. Dis. *5,* 37–45.

Gibson, G.E., Zhang, H., Toral-Barza, L., Szolosi, S., and Tofel-Grehl, B. (1996). Calcium stores in cultured fibroblasts and their changes with Alzheimer's disease. Biochim. Biophys. Acta *1316,* 71–77.

Grudt, T.J., Usowicz, M.M., and Henderson, G. (1996). Ca^{2+} entry following store depletion in SH-SY5Y neuroblastoma cells. Mol. Brain Res. *36,* 93–100.

Guo, Q., Furukawa, K., Sopher, B.L., Pham, D.G., Xie, J., Robinson, N., Martin, G.M., and Mattson, M.P. (1996). Alzheimer's PS-1 mutation perturbs calcium homeostasis and sensitizes PC12 cells to death induced by amyloid β-peptide. Neuroreport *8,* 379–383.

Hofer, A.M., Fasolato, C., and Pozzan, T. (1998). Capacitative Ca^{2+} entry is closely linked to the filling state of internal Ca^{2+} stores: a study using simultaneous measurements of I_{CRAC} and intraluminal. J. Cell Biol. *140,* 325–334.

Hoth, M., and Penner, R. (1992). Depletion of intracellular calcium stores activates a calcium current in mast cells. Nature *355,* 353–356.

Irvine, R.F. (1990). "Quantal" Ca^{2+} release and the control of Ca^{2+} entry by inositol phosphate—a possible mechanism. FEBS Lett. *263,* 5–9.

Ito, E., Oka, K., Etcheberrigaray, R., Nelson, T., McPhie, D.L., Tofel-Grehl, B., Gibson, G.E., and Alkon, D.L. (1994). Internal Ca^{2+}-mobilization is altered in fibroblasts from patients with Alzheimer's disease. Proc. Natl. Acad. Sci. USA *91,* 534–538.

Iwatsubo, T., Odaka, A., Suzuki, N., Mizusawa, H., Nukina, N., and Ihara, Y. (1994). Visualization of Aβ42(43) and Aβ40 in senile plaques with end-specific Aβ monoclonals: evidence that an initially deposited species is Aβ42(43). Neuron *13,* 45–53.

Janicki, S., and Monteiro, M.J. (1997). Increased apoptosis arising from increased expression of the Alzheimer's disease-associated presenilin-2 mutation (N141I). J. Cell Biol. *139*, 485–495.

Jayadev, S., Petranks, J.G., Cheran, S.K., Biermann, J.A., Barret, J.C., and Murphy, E. (1999). Reduced capacitative calcium entry correlates with vesicle accumulation and apoptosis. J. Biol. Chem. *274,* 8261–8268.

Johnson-Wood, K., Lee, M., Motter, R., Hu, K., Gordon, G., Barbour, R., Khan, K., Gordon, M., Tan, H., Games, D., et al. (1997). Amyloid precursor protein processing and $A\beta_{42}$ deposition in a transgenic mouse model of Alzheimer's disease. Proc. Natl. Acad. Sci. USA *94,* 1550–1555.

Katayama, T., Imaizumi, K., Sato, N., Miyoshi, K., Kudo, T., Hitomi, J., Morihara, T., Yoneda, T., Gomi, F., Mori, Y., et al. (1999). Presenilin-1 mutations downregulate the signaling pathway of the unfolded-protein response. Nat. Cell Biol. *1,* 479–485.

Kerschbaum, H.H., and Cahalan, M.D. (1999). Single-channel recording of a store-operated Ca^{2+} channel in Jurkat T lymphocytes. Science *283,* 836–839.

Kim, T.-W., Pettingell, W.H., Hallmark, O.G., Moir, R.D., Wasco, W., and Tanzi, R.E. (1997). Endoproteolytic processing and proteasomal degradation of presenilin 2 in transfected cells. J. Biol. Chem. *272,* 11006–11010.

Kim, S.H., Lah, J.S., Thinakaran, G., Levey, A., and Sisodia, S. (2000). Subcellular localization of presenilins: association with a unique membrane pool in cultured cells. Neurobiol. Dis. *7,* 99–117.

Kimberly, W.T., Xia, W., Rahmati, T., Wolfe, M.S., and Selkoe, D.J. (2000). The transmembrane aspartate in presenilin 1 and 2 are obligatory for γ-secretase activity and amyloid β-protein generation. J. Biol. Chem. *275,* 3173–3178.

Kiselyov, K., Xu, X., Mozhayeva, G., Kuo, T., Pessah, I., Mignery, G., Zhu, X., Birnbaumer, L., and Muallem, S. (1998). Functional interaction between $InsP_3$ receptors and store-operated Htrp3 channels. Nature *396,* 478–482.

Kiselyov, K., Mignery, G.A., Zhu, M.X., and Muallem, S. (1999). The N-terminal domain of the IP_3 receptor gates store-operated hTRP3 channels. Mol. Cell *4,* 423–429.

Kovacs, D.M., Fausett, H.J., Page, K.J., Kim, T.-W., Moir, R.D., Merriam, D.E., Hollister, R.D., Hallmark, O.G., Mancini, R., Felsenstein, K.M., et al. (1996). Alzheimer associated presenilins 1 and 2: neuronal expression in brain and localization to intracellular membranes in mammalian cells. Nat. Med. *2,* 224–229.

Leissring, M.A., Parker, I., and LaFerla, F.M. (1999). Presenilin-2 mutations modulate amplitude and kinetics of inositol 1,4,5-triphosphate-mediated calcium signaling. J. Biol. Chem. *274,* 32535–32538.

Li, X., and Greenwald, I. (1998). Additional evidence for an eight transmembrane-domain topology for Caenorhabditis elegans and human presenilin. Proc. Natl. Acad. Sci. USA *95,* 7109–7114.

Li, H.-S., Xu, X.-Z.S., and Montell, C. (1999). Activation of a TRPC3-dependent cation current through the neurotrophin BDNF. Neuron *24,* 261–273.

Lin, X., Antalffy, B., Kang, D., Orr, H.T., and Zoghbi, H.Y. (2000). Polyglutamine expansion downregulates specific neural genes before pathologic changes in SCA1. Nat. Neurosci. *3,* 157–163.

Ma, H.-T., Patterson, R.L., van Rossum, D.B., Birnbaumer, L., Mikoshiba, K., and Gill, D.L. (2000). Requirement of the inositol triphosphate receptor for activation of store-operated Ca^{2+} channels. Science *287,* 1647–1651.

Mason, M.J., Mayer, B., and Hymel, L.J. (1993). Inhibition of Ca^{2+} transport pathways in thymic lymphocytes by econazole, miconazole and SKF 96365. Am. J. Physiol. *264,* C564–C662.

Meldolesi, J., and Pozzan, T. (1998). The endoplasmic reticulum Ca^{2+} store: a view from the lumen. Trends Biol. Sci. *23,* 10–14.

Merritt, J.E., Armstrong, W.P., Benham, C.D., Hallam, T.J., Jacob, R., Jaxa-Chamiec, A., Leigh, B.K., McCarthy, S.A., Moores, K.E.,

and Rink, T.J. (1990). SK&F 96365, a novel inhibitor of receptor-mediated calcium entry. Biochem. J. *271,* 515–522.

Mignen, O., and Shuttleworth, T.J. (2000). I_{ARC}, a novel arachidonate-regulated, noncapacitative Ca^{2+} entry channel. J. Biol. Chem. *275,* 9114–9119.

Naruse, S., Thinakaran, G., Luo, J.-J., Kusiak, J.W., Tomita, T., Iwatsubo, T., Qian, X., Ginty, D.D., Price, D.L., Borchelt, D.R., et al. (1998). Effects of PS1 deficiency on membrane protein trafficking in neurons. Neuron *21,* 1213–1221.

Niwa, M., Sidrauski, C., Kaufman, R.J., and Walter, P. (1999). A role for presenilin-1 in nuclear accumulation of Ire1 fragments and induction of the mammalian unfolded protein response. Cell *99,* 691–702.

Oyama, F., Sawamura, N., Kobayashi, K., Morishima-Kawashima, M., Kuramochi, T., Ito, M., Tomita, T., Maruyama, K., Saido, T.C., Iwatsubo, T., et al. (1998). J. Neurochem. *71*, 313–322.

Pack-Chung, E., Meyers, M.B., Pettingell, W.P., Moir, R.D., Brownawell, A.M., Cheng, I., Tanzi, R.E., and Kim, T.-W. (2000). Presenilin 2 interacts with sorcin, a modulator of the ryanodine receptor. J. Biol. Chem. *275,* 14440–14445.

Patterson, R.L., van Rossum, D.B., and Gill, D.L. (1999). Store-operated Ca^{2+} entry: evidence for a secretion-like coupling model. Cell *98,* 487–499.

Philipp, S., Wissenbach, U., and Flockerzi, V. (2000). The molecular biology of calcium channels. In Calcium Signaling, J.W. Putney, Jr., ed. (Boca Raton, FL: CRC Press), pp. 321–342.

Putney, J.W., Jr. (1986). A model for receptor-regulated calcium entry. Cell Calcium *7,* 1–12.

Putney, J.W., Jr. (1990). Capacitative calcium entry revisited. Cell Calcium *11,* 611–624.

Putney, J.W., Jr. (1999a). "Kissin' cousins": intimate plasma membrane-ER interactions underlies capacitative calcium entry. Cell *99,* 5–8.

Putney, J.W., Jr. (1999b). TRP, inositol 1,4,5-triphosphate receptors, and capacitative calcium entry. Proc. Natl. Acad. Sci. USA *96,* 14669–14671.

Ribeiro, C.M.P., Reece, J., and Putney, J.W. (1997). Role of the cytoskeleton in calcium signaling in NIH 3T3 cells: an intact cytoskeleton is required for agonist-induced $[Ca^{2+}]_i$ signaling, but not for capacitative calcium entry. J. Biol. Chem. *272,* 26555–26561.

Saura, C.A., Tomita, T., Davenport, F., Harris, C.L., Iwatsubo, T., and Thinakaran, G. (1999). Evidence that intramolecular associations between presenilin domains are obligatory for endoproteolytic processing. J. Biol. Chem. *274,* 13818–13823.

Scheuner, D., Eckman, C., Jensen, M., Song, X.M., Citron, M., Suzuki, N., Bird, T.D., Hardy, J., Hutton, M., Kukull, W., et al. (1996). Aβ42(43) is increased in vivo by the PS1/2 and APP mutations linked to familial Alzheimer's disease. Nat. Med. *2,* 864–870.

Seeger, M., Nordstedt, C., Petanceska, S., Kovacs, D.M., Gouras, G.K., Hahne, S., Fraser, P., Levesque, L., St. Czernik, A.J., George-Hyslop, P., et al. (1997). Evidence for phosphorylation and oligomeric assembly of presenilin 1. Proc. Natl. Acad. Sci. USA *94*, 5090–5094.

Selkoe, D.J. (1998). The cell biology of β-amyloid precursor protein and presenilin in Alzheimer's disease. Trends Cell Biol. *8,* 447–453.

Selkoe, D.J. (2000). Notch and presenilins in vertebrates and invertebrates: implications for neuronal development and degeneration. Curr. Opin. Neurobiol. *10*, 50–57.

Shen, J., Bronson, R.T., Chen, D.F., Xia, W., Selkoe, D.J., and Tonegawa, S. (1997). Skeletal and CNS defects in presenilin-1-deficient mice. Cell *89,* 629–639.

Shuttleworth, T.J. (1996). Arachidonic acid activates the noncapacitative entry of Ca^{2+} during $[Ca^{2+}]_i$ oscillations. J. Biol. Chem. *271,* 21720–21725.

Steiner, H., Duff, K., Capell, A., Romig, H., Grim, M.G., Lincoln, S., Hardy, J., Yu, X., Picciano, M., Fechteler, K., et al. (1999). A loss of function mutation of presenilin-2 interferes with amyloid β-peptide production and Notch signaling. J. Biol. Chem. *274,* 28669–28673.

Struhl, G., and Greenwald, I. (1999). Presenilin is required for activity and nuclear access of Notch in Drosophila. Nature *398,* 522–525.

Tanzi, R.E. (1998). The molecular genetics of Alzheimer's disease. In Scientific American Molecular Neurology, J.B. Martin, ed. (New York, NY: Scientific American Press), pp. 55–75.

Thinakaran, G., Borchelt, D., Lee, M., Slunt, H., Spitzer, L., Kim, G., Ratovitsky, T., Davenport, F., Nordstedt, C., Seeger, M., et al. (1996). Endoproteolysis of presenilin 1 and accumulation of processed derivatives in vivo. Neuron *17,* 181–190.

Thinakaran, G., Harris, C.L., Ratovitski, T., Davenport, F., Slunt, H.H., Price, D.L., Borchelt, D.R., and Sisodia, S.S. (1997). Evidence that levels of presenilins (PS1 and PS2) are coordinately regulated by competition for limiting cellular factors. J. Biol. Chem. *272,* 28415–28422.

Thinakaran, G., Regard, J.B., Bouton, C.M.L., Harris, C.L., Price, D.L., Borchelt, D.R., and Sisodia, S.S. (1998). Stable association of presenilin derivatives and absence of presenilin interactions with APP. Neurobiol. Dis. *4,* 438–453.

Tomita, T., Maruyama, K., Saido, T.C., Kume, H., Shinozaki, K., Tokuhiro, S., Capell, A., Walter, J., Grünberg, J., Haass, C., et al. (1997). The presenilin 2 mutations (N141I) linked to familial Alzheimer disease (Volga German families) increases the secretion of amyloid β protein ending at the 42nd (or 43rd) residue. Proc. Natl. Acad. Sci. USA *94*, 2025–2030.

Tomita, T., Takikawa, R., Koyama, A., Morohashi, Y., Takasugi, N., Saido, T.C., Maruyama, K., and Iwatsubo, T. (1999). C terminus of presenilin 1 is required for overproduction of amyloidogenic Aβ42 through stabilization and endoproteolysis of presenilin. J. Neurosci. *19*, 10627–10634.

Vazquez, G., de Boland, A.R., and Boland, R.L. (1998). 1-alpha,25-dihydroxy-vitamin-D3-induced store-operated Ca^{2+} influx in skeletal muscle cells: modulation by phospholipase c, protein kinase c, and tyrosine kinases. J. Biol. Chem. *273,* 33954–33960.

Waldron, R.T., Short, A.D., and Gill, D.L. (1997). Store-operated Ca^{2+} entry and coupling to Ca^{2+} pool depletion in thapsigargin-resistant cells. J. Biol. Chem. *272,* 6440–6447.

Wolfe, M.S., Xia, W., Ostaszewski, B.L., Diehl, T.S., Kimberly, W.T., and Selkoe, D.J. (1999). Two transmembrane aspartates in presenilin-1 required for presenilin endoproteolysis and γ-secretase activity. Nature *398,* 513–517.

Wolozin, B., Iwasaki, K., Vito, P., Ganjei, K., Lacana, E., Sunderland, T., Zhao, B., Kusiak, J.W., Wasco, W., and D'Adamio, L. (1996). PS2 participates in cellular apoptosis: constitutive activity conferred by Alzheimer mutation. Science *274,* 1710–1713.

Xia, W., Zhang, J., Kholodenko, D., Citron, M., Podlisney, M.B., Teplow, D.B., Haass, C., Seubert, P., Koo, E.H., and Selkoe, D.J. (1997). Enhanced production and oligonerization of the 42-residue amyloid beta protein by Chinese hamster ovary cells stably expressing mutant presenilins. J. Biol. Chem. *272,* 7977–7982.

Yao, Y., Ferrer-Montiel, A.V., Montal, M., and Tsien, R.Y. (1999). Activation of store-operated Ca^{2+} current in *Xenopus* oocytes requires SNAP-25 but not a diffusible messenger. Cell *98,* 475–485.

Ye, Y., Lukinova, N., and Fortini, M.E. (1999). Neurogenic phenotypes and altered Notch processing in Drosophila presenilin mutants. Nature *398,* 525–529.

Yoo, A.S.J., Krieger, C., and Kim, S.U. (1999). Process extension and intracellular Ca^{2+} in cultured murine oligodendrocytes. Brain Res. *827,* 19–27.

Zhu, X., Jiang, M., Peyton, M., Boulay, G., Hurst, R., Stefani, E., and Birnbaumer, L. (1996). *trp*, a novel mammalian gene family essential for agonist-activated capacitative Ca^{2+} entry. Cell *85,* 661–671.

Zweifach, A., and Lewis, R.S. (1993). Mitogen-regulated Ca^{2+} current of T lymphocytes is activated by depletion of intracellular Ca^{2+} stores. Proc. Natl. Acad. Sci. USA. *90,* 6295–6299.